Science of the Total Environment 475 (2014) 29–38

Contents lists available at ScienceDirect

Science of the Total Environment

journal homepage: www.elsevier.com/locate/scitotenv

Mass and number size distributions of particulate matter components: Comparison of an industrial site and an urban background site

Adewale M. Taiwo, David C.S. Beddows, Zongbo Shi, Roy M. Harrison *

Division of Environmental Health & Risk Management, School of Geography, Earth & Environmental Sciences, University of Birmingham, Edgbaston, Birmingham B15 2TT, United Kingdom

HIGHLIGHTS

- Size distribution of major ions and trace metals is reported.
- Comparison is made between an industrial (steelworks) site and urban background.
- The steelworks impacts heavily upon coarse mode mass and concentration of Ca, Mg, K, Fe, and Mn.
- Steelworks site also shows elevated Zn and Cr.
- Concentrations of traffic-associated metals (especially Ba, Sb, Cu and Pb) are greatest at urban background.

GRAPHICAL ABSTRACT

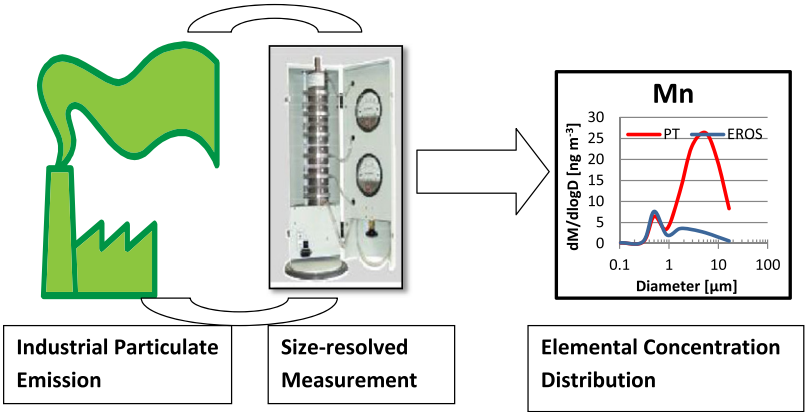

ARTICLE INFO

Article history:
Received 4 July 2013
Received in revised form 28 November 2013
Accepted 16 December 2013
Available online 11 January 2014

Keywords:
Particle size distribution
Chemical composition
Urban background
Steelworks
Impactor

ABSTRACT

Size-resolved composition of particulate matter (PM) sampled in the industrial town of Port Talbot (PT), UK was determined in comparison to a typical urban background site in Birmingham (EROS). A Micro-Orifice Uniform Deposit Impactor (MOUDI) sampler was deployed for two separate sampling campaigns with the addition of a Grimm optical spectrometer at the PT site. MOUDI samples were analysed for water-soluble anions (Cl^-, NO_3^- and SO_4^{2-}) and cations (Na^+, NH_4^+, K^+, Mg^{2+} and Ca^{2+}) and trace metals (Al, V, Cr, Mn, Fe, Cu, Zn, Sb, Ba and Pb). The PM mass distribution showed a predominance of fine particle ($PM_{2.5}$) mass at EROS whereas the PT samples were dominated by the coarse fraction ($PM_{2.5\text{-}10}$). SO_4^{2-}, Cl^-, NH_4^+, Na^+, NO_3^-, and Ca^{2+} were the predominant ionic species at both sites while Al and Fe were the metals with highest concentrations at both sites. Mean concentrations of Cl^-, Na^+, K^+, Ca^{2+}, Mg^{2+}, Cr, Mn, Fe and Zn were higher at PT than EROS due to industrial and marine influences. The contribution of regional pollution by sulphate, ammonium and nitrate was greater at EROS relative to PT. The traffic signatures of Cu, Sb, Ba and Pb were particularly prominent at EROS. Overall, PM at EROS was dominated by secondary aerosol and traffic-related particles while PT was heavily influenced by industrial activities and marine aerosol. Profound influences of wind direction are seen in the 72-hour data, especially in relation to the PT local sources. Measurements of particle number in 14 separate size bins plotted as a function of wind direction and speed are highly indicative of contributing sources, with local traffic dominant below 0.5 μm, steelworks emissions from 0.5 to 15 μm, and marine aerosol above 15 μm.

* Corresponding author. Also at: Department of Environmental Sciences/Center of Excellence in Environmental Studies, King Abdulaziz University, Jeddah 21589, Saudi Arabia. Tel.: +44 121 414 3494.
E-mail address: r.m.harrison@bham.ac.uk (R.M. Harrison).

0048-9697/$ – see front matter
http://dx.doi.org/10.1016/j.scitotenv.2013.12.076

1. Introduction

Particulate matter is commonly classified in three modes namely ultrafine (nucleation and Aitken mode, diameter less than 0.1 μm), fine (mainly accumulation mode, aerodynamic diameter between 0 and 2.5 μm) and coarse (aerodynamic diameter between 2.5 and 10 μm). Generally, fine and ultrafine PM are formed from high temperature processes such as vehicular exhaust, oil and coal combustion, biomass burning, industrial processes, and chemical reactions in the atmosphere (Harrison et al., 2003a; Samara et al., 2003). Coarse particles are generally evolved from attrition processes including mechanical abrasion of crustal material and re-suspension of road and soil dusts, sea spray, volcanic eruptions and brake and tyre wear from vehicles (Allen et al., 2001).

Atmospheric PM is made up of diverse chemical substances including water soluble ions, trace metals and organic compounds. Water-soluble ions constitute a significant portion of PM mass (Yin and Harrison, 2008)., and therefore play an important role in aerosol chemistry. Sulphate and nitrate are formed mainly from oxidation of SO_2 and NO_x. Sodium, magnesium and chloride are the main components of sea spray; potassium arises from biomass burning or soil and Ca from construction, soil and steelworks emissions (Oravisjarvi et al., 2003; Pandolfi et al., 2011). A number of anthropogenic, geogenic and biogenic activities are responsible for emissions of trace metals into the atmospheric environment and hence play important roles in determining size distributions (Allen et al., 2001). Each has a characteristic size distribution reflective of its source.

The Micro-Orifice Uniform Deposit Impactor (MOUDI) has been widely used for particle size measurement in both indoor and outdoor pollution studies. These studies have reported PM size distributions for water soluble and trace metal components (Allen et al., 2001; Cabada et al., 2004; Harrison et al., 2003a; Chang et al., 2008; Dall'Osto et al., 2008; Liu et al., 2008; Zhao and Gao, 2008; Gietl et al., 2010; Ny and Lee, 2011). Na, Cl, Ca and Al typically show modes in the coarse fraction while Cd, Zn, Mn, Ni and Cu have modes in the fine fraction (Ny and Lee, 2011). Allen et al. (2001) reported MOUDI data for trace metals from three urban background sites in the UK. Dall'Osto et al. (2008) employed a MOUDI for particle size-resolved measurements at a steel industry site in the UK. Water-soluble ions in particulate matter, from nanoparticles to the coarse mode have been determined with a MOUDI and nano-MOUDI in Taiwan by Chang et al. (2008). In London, particle size-segregated aerosol has been measured at roadside and background sites by Gietl et al. (2010). PM size-segregation and associated metallic elements in an industrialized city in Korea have been reported (Ny and Lee, 2011). None of these studies have compared the size distribution of PM and its components collected at urban background and industrial (especially steelworks) locations for both water soluble ions and trace metals. In this study, particle size distributions of both ionic species and trace metals at typical background and industrial sites were studied, offering an opportunity for identifying source signatures of components contributing to PM in the atmosphere of the two study areas. The results add to a relatively small international database of mass size distributions for specific chemical components, and highlight the very different sources of particulate matter at the two sites. Additionally, particle number spectra from 0.3 μm to >15 μm are reported and analysed according to wind speed and direction.

2. Materials and methods

2.1. The study areas

2.1.1. Port Talbot (PT)

PT is a coastal industrial town with a population of approximately 35,000 and located on the M4 corridor in South Wales (51° 34′ N and 3° 46′ W). The Tata steel complex located in Port Talbot town is the main industry in the study area and a major source of PM emissions (AQEG, 2011). The site covers approximately 28 km^2, comprises of ~50 km of roads, 100 km of railway, and 25,000 vehicle movements per day. The production capacity is around 5 m tonnes per year with the main processes in the steelworks being iron-making (sintering, blast furnace and raw materials), steel-making (basic oxygen steel-making (BOS) and coking) and rolling mills (hot and cold mills) (Moreno et al., 2004; Dall'Osto et al., 2008). The location of the sampling site (Fire Station) is shown in Fig. 1.

2.1.2. Elms Road Observatory Site (EROS)

EROS (1.93°W; 52.46°N) is a typical suburban background site located in an open field within the University of Birmingham campus. The site is about 3.5 km southwest of the centre of Birmingham (population of over one million and part of a conurbation of 2.5 million population (Yin et al., 2010). The EROS study site is shown in Fig. 2. The nearest roads are lightly trafficked and the nearby railway line carries mainly electric trains.

2.2. Particulate matter sampling

Size-fractionated particle sampling was carried out with 8-stage MOUDI™ (Model 100) having cut points of 10, 5.6, 3.2, 1.8, 1.0, 0.56, 0.32 and 0.18 μm, and a nominal flow of rate 30 L/min. As a flow rate of 21.5 L/min was achieved throughout the sampling periods at both sites, a correction factor was applied using the formula: $Dp \times \sqrt{(F1/F2)}$ where Dp is the MOUDI stage nominal cut-point, F1 is the design flow rate of the MOUDI (30 L/min) while F2 is the achieved flow rate during the campaign (21.5 L/min). Polytetrafluoroethylene (PTFE) filters (Whatman, diameter 47 mm and pore size 1.0 μm) were used for particle collection on all the impaction stages while quartz filters (Whatman, diameter 37 mm) were used as backups. At EROS, a total of four MOUDI 72 hour-samples were generated during the sampling period between March 30 and April 11. At the PT sampling site, ten MOUDI samples of 72 h each were collected during a one month sampling campaign that started on April 17 and ended on May 16, 2012. The tenth sample was collected for just 36 h. Prior to sampling and after sampling, all filters were weighed with a Sartorius microbalance (Model MC 5; 1 μg sensitivity) equipped with a Polonium-210 anti-static source having been subjected to at least 24 h pre-conditioning (20 ± 5 °C and 50 ± 10% R.H.) in our clean weighing room.

2.3. Meteorological conditions

Average wind speed and temperature at the Birmingham (Tyburn) and Port Talbot (Fire Station) Automatic Urban Rural Network (AURN) sites were calculated (http://uk-air.defra.gov.uk/networks/aurn-site-info). The AURN station at Birmingham, Tyburn was used to represent the EROS site. During the period of sampling at EROS (March 30–April 11), the average wind speed and temperature were 4.3 ± 1.8 m s^{-1} and 6.7 ± 1.4 °C respectively. At PT where the sampling campaign took place between April 17 and May 16, the values were 6.3 ± 2.3 m s^{-1} and 8.6 ± 1.4 °C.

2.4. Sample digestion and analysis

Exposed filters were cut into two equal halves. One half was analysed for water-soluble ions (Na^+, Mg^{2+}, Ca^{2+}, K^+, NH_4^+, Cl^-, NO_3^-, SO_4^{2-}) while the second half was analysed for trace metals (Al, V, Cr, Mn, Fe, Cu, Zn, Sb, Ba and Pb). Blank filters were also analysed and subtracted from the exposed filter data.

Filter samples for ionic species analysis were extracted with 7.5 mL distilled de-ionised water (DDW, conductivity of 18.2 MΩ) with agitation on a mechanical shaker (Model IKA Labortechnik KS 250 basic) set at 240 rpm for a period of 40 min. Prior to addition of DDW and shaking, PTFE filters were first treated with 0.3 mL propan-2-ol to wet the surface. The extracts were analysed with a Dionex DX 500 and

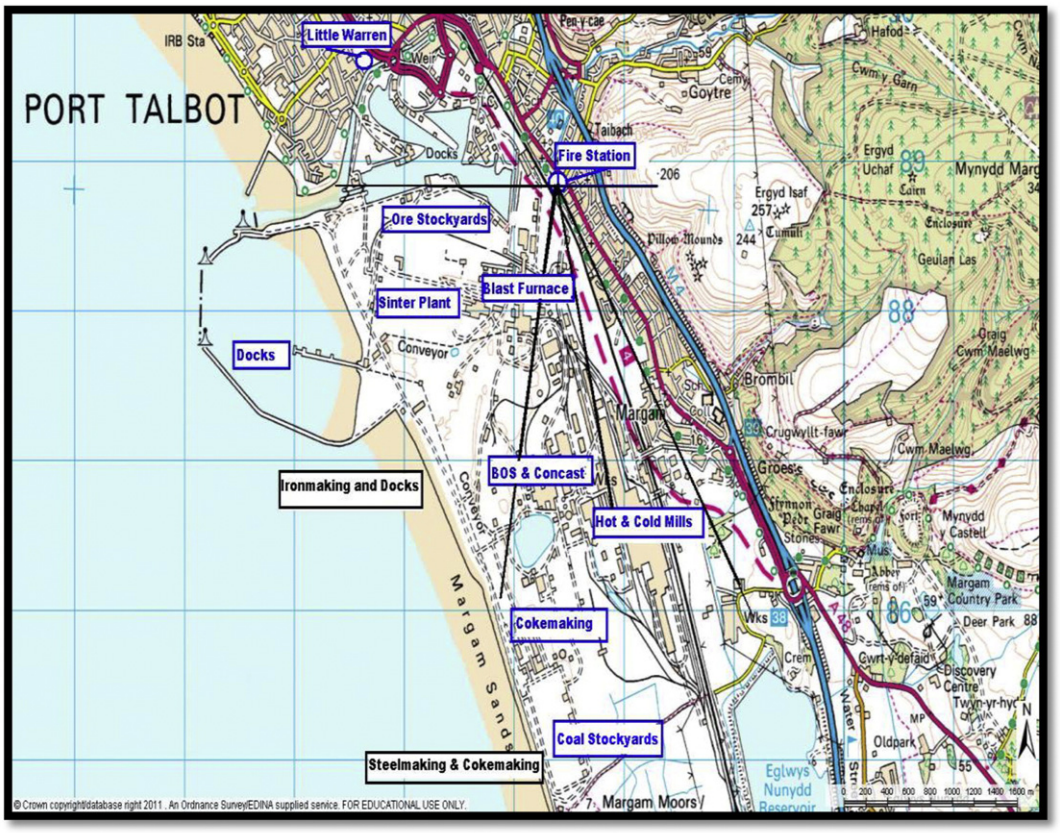

© Crown Copyright/database right 2011. An Ordnance Survey EDINA supplied service.

Fig. 1. Port Talbot sampling station and the steelworks processing units.

Map data: Google Earth 2010 (http://www.google.com)

Fig. 2. The map of EROS located within the University of Birmingham campus, Birmingham, UK.

ICS-2000 Ion Chromatography (IC) system for cations and anions respectively. Eluants used were methane sulphonic acid (MSA) and KOH for cation and anion IC instruments, respectively. Detailed procedures for the Dionex analysis have been described by Yin et al. (2010).

The second half of the exposed filters was extracted with dilute reverse *aqua regia* (2.23 M HCl and 1.03 M HNO_3) following the procedure of Harrison et al. (2003b). The mixed acid extractant (2 mL) was added to the filters placed inside 4 mL narrow neck bottles and heated at 100 °C for 30 min in a water bath and then placed in an ultrasonic bath at 50 °C for another 30 min. This cycle was repeated and the resulting digests transferred into 15 mL narrow neck bottles and rinsed with 10 mL distilled deionised water. The extracts were then analysed by Inductively Coupled Plasma Mass Spectrometry (ICPMS, Agilent 7500 Ce). Mixed standards (from stock 1000 mg/L VWR standard solutions) were prepared in the series 0, 1, 5, 10, 20, 50 and 100 ppb. Internal standards employed by the ICPMS instrument were Sc, Ge, Y, In and Bi.

In earlier work, this procedure has been evaluated by analysis of NIST SRM 1684a (Allen et al., 2001) and more recent trials have shown high efficiency (<85%) for all elements analysed except Al (*ca* 50% efficiency, also by comparison with XRF) and Cr (*ca* 50% efficiency). Since extraction efficiency may vary according to particle size, this may introduce bias into the size distributions reported for these elements.

2.5. Number size distributions

Particle number size spectra in the range 0.3 to 20 μm were measured at the Port Talbot site using a Grimm model #1.108 optical particle spectrometer which measures the intensity of light scattered at 90 °C to a beam produced by a laser diode. Particles are classified into 14 size fractions between the smallest (0.3–0.4) and the largest (15–20 μm) bins.

3. Results and discussion

3.1. MOUDI particle size distributions

3.1.1. Port Talbot

Fig. S1 represents the temporal variations of MOUDI data for mass and ionic components from the industrially influenced PT site. Bimodal peaks (0.5 and 2–6 μm) were observed for mass distribution for each MOUDI sample during the campaign with highest mass concentration observed on April 23–26 which coincided with the start of a PM_{10} episode on April 26th reaching hourly concentrations in excess of 100 μg m^{-3}. Most of the water soluble components displayed two distinct modal peaks in the fine mode except Cl^- (other than the May 11–14 sample which showed two modal peaks), NH_4^+ and Ca^{2+}. Common fine modal peaks of 0.5 μm and coarse modal peaks of 2–6 μm were observed for most of the ionic species except for K^+ which showed diverse modal peaks in various sampling periods, suggesting multiple sources of K^+ in Port Talbot. However, the common peak at 0.5 μm shown by K^+ in all the samples indicated a common emission source for which biomass combustion or steelworks activities are the major suspects. An episode of Ca^{2+}, Cl^-, and NO_3^- was observed between May 2 and May 5 all showing higher concentrations at 3.0 μm. This was also observed for ammonium and sulphate with a peak at 0.5 μm. Elevated Ca^{2+} observed during this episode might have sources either from construction activities or steelworks emissions. In the blast furnace of the steelworks, limestone ($CaCO_3$) and dolomite ($CaMg(CO_3)_2$) are used as fluxing agents while in the basic oxygen furnace (BOF) section, lime (CaO) and fluorspar (CaF_2) are fluxing raw materials (Machemer, 2004). The MOUDI sample of April 20–23 showed higher concentrations of Cl^-, Na^+ and Mg^{2+} all peaking in the particle size range 3–5 μm. This typifies a sea spray episode.

Fig. S2 shows the trace metal size distribution of MOUDI samples during the one-month campaign. The concentration of Fe was the highest, followed by Al (may be underestimated as mentioned above) and Zn. All the metal data show two or more modal peaks covering the fine and coarse particle ranges except Pb and Zn which have their modes in the fine fraction only (0.5 and 1–2 μm). Mn and Fe showed similar modes throughout the sampling periods suggesting common emission sources. In the fine mode, most of the trace metals peak at 0.5 μm except for the April 26–29 sample which showed exceptional elevated peaks for Cr and Cu at 0.2–0.3 μm. Combustion of copper chrome arsenate (CCA) treated wood could explain the unusual peaks of these trace metals on these days. CCA was used as a wood preservative before its ban in the UK in 2007 (Wood Protection Association, 2010). However, CCA treated wood may still remain in many structures. Despite the fact that Cu is often a good marker for traffic (brake dust), its appearance at 0.2–0.3 μm is not consistent with traffic as other traffic markers such as Sb and Ba were peaking at a different diameter (0.5 μm). Additionally, in the size range 1–2 μm significant amounts of Al and V appeared in the April 26–29 MOUDI sample. Apart from this date, V peaked at 0.5 μm throughout; but Al showed different fine modal peaks at 0.2–0.3, 0.5 and 1–2 μm. Al in the fine mode could arise from vehicular, coal combustion and metallurgical activities (Kleeman et al., 2000; Xia and Gao, 2010) while fine V normally arises from fuel/oil combustion and shipping emissions (Figueroa et al., 2006; Pandolfi et al., 2011). The appearance of irregular peaks on April 26–29 implies that Al and V could arise from the same sources that emitted Cu and Cr into the atmosphere. The wind rose for that sampling interval (see Fig. S5 in Supplementary information) indicates that the source is unlikely to be associated with the steelworks.

3.1.2. EROS

Individual 72-h MOUDI size segregated mass and water soluble ion distributions from the EROS site are represented in Fig. S3. The gravimetric mass showed modal peaks in the fine and coarse PM ranges at 0.5 μm and 2–4 μm. Among the water soluble ions, Cl^-, Na^+, Mg^{2+} and Ca^{2+} depicted a unimodal peak at 3–6 μm. Ammonium exhibited a single peak in the fine mode (0.5 μm). Other ionic species showed bimodal behaviour generally peaking at 0.5 and 3 μm except in the April 8–11 sample where NO_3^- peaked at a single mode of 1–2 μm. A sulphate coarse mode occurred at around 5.0 μm. Among the ionic components of PM, sulphate constituted the highest concentration while $K^+ < Mg^{2+} < Ca^{2+}$ were the ionic species of lowest abundance.

MOUDI trace metal size distributions at the EROS sampling site are shown in Fig. S4. Unlike water soluble ions where the highest concentrations were observed in the March 30–April 2 sample, metal concentrations were higher on April 5–8. All of the metals displayed at least two peaks covering fine and coarse PM fractions except Pb, Zn, and Sb where the two modes were both in the fine fraction, other than in the sample collected on April 8–11 which displayed a coarse mode peak at 2–3 μm for Sb. Multiple modes were observed for Al, V and Cr (0.5, 1–2, 3 and 10 μm). On March 30–April 2, V, Cr, Cu, Zn, Sb and Pb all showed similar peaks at fine modes of 0.5 and 1–2 μm indicating possible emissions from traffic and industrial combustion processes (Zanobetti et al., 2009). Zn measured on April 5–8 showed a coarse modal peak which might be linked with traffic emissions of brake or tyre dust (Harrison et al., 2012a). Different peaks exhibited by the measured metals during different sampling periods suggested diverse emission sources.

3.2. Comparison of average MOUDI size distributions from EROS and PT

A summary of the source assignments and modes in the size distributions appears in Table 1.

Fig. 3 shows the average size distribution data for mass, water soluble ions and trace metal concentrations at EROS and PT sites. Different patterns were observed for these particle constituents. At both sites, mass concentrations, Na^+, K^+, Fe, Cu and Ba exhibited two modal peaks generally occurring at 0.5–0.6 μm and at 2–6 μm. Average mass concentrations showed a slight elevation of fine particle mass at EROS while an elevated concentration of coarse particles was evident at PT

Table 1
Sources and modes of the constituents analysed at the Port Talbot (PT) and EROS sites.

Component	Modes	Major/minor sources	Site
Cl^-	C	Sea salt (major)	PT, EROS
	F	NH_4Cl (minor)	PT
NO_3^-	C	Sodium nitrate (major)	PT, EROS
	F	NH_4NO_3 (minor)	PT, EROS
SO_4^{2-}	F	$(NH_4)_2SO_4$ (major)	PT, EROS
	C (1,2)	Sea salt (minor)	PT, EROS
Na^+	C	Sea salt (major)	PT, EROS
	F		PT
NH_4^+	F	$(NH_4)_2SO_4$; NH_4NO_3 (major)	PT, EROS
K^+	F	Woodsmoke (major)	PT, EROS
	C(1)	Sea salt, soil (minor)	PT, EROS
	C(2)	Steelworks (minor)	PT
Mg^{2+}	C	Sea salt (major)	PT, EROS
	F	Steelworks (minor)	PT
Ca^{2+}	C	Crustal, steelworks (major)	PT, EROS
	F	Steelworks (minor)	PT
Al	F	Crustal/soil	PT, EROS
	C		PT, EROS
V	F	Fuel oil (major)	PT, EROS
	C		PT, EROS
Cr	F, C	Steelworks and other	PT, EROS
Mn	C	Steelworks (major)	PT, EROS
	F	Steelworks (minor)	PT, EROS
Fe	C	Steelworks (major), brake wear (major)	PT, EROS
	F	Steelworks (minor)	PT, EROS
Cu	C	Brake wear (major)	PT, EROS
	F	Steelworks (minor)	PT, EROS
Zn	C	Tyre wear, steelworks	PT, EROS
	F	Tyre wear, steelworks	PT, EROS
Sb	C	Brake wear	PT, EROS
	F	Brake wear	PT, EROS
Ba	C	Brake wear	PT, EROS
	F	Brake wear	EROS
Pb	F	Steelworks	PT, EROS
	C		PT, EROS

Note: C = coarse; F = fine.
Attribution of a mode to the steelworks applies to the PT site only.

relative to the other sites. Meteorological conditions, especially wind speed and temperature are known to influence particle concentration and size distributions (Charron and Harrison, 2005; Jones et al., 2010). During dry and windy conditions, elevated amounts of coarse particles could be favoured due to re-suspension of soil, road and industrial dusts.

Generally, the modes in the size distributions were similar at the two sites (Fig. 3). Notable differences in the modes were as follows:

- calcium showed a fine mode at PT which was not evident at EROS. This may be an emission from the steel industry.
- aluminium showed a pronounced mode >10 μm at EROS which has no parallel at PT, and probably arises from resuspension of road dust (Harrison et al., 2012a).
- chromium shows a multi-modal behaviour at both sites, but the smallest mode at PT is at around 0.2 μm, whereas at EROS it is close to 0.5 μm. Either steelworks emissions or combustion of wood treated with copper chrome arsenate (CCA) preservative may be the source.
- manganese, for which PT shows a very pronounced coarse particle mode at *ca* 5 μm, while at EROS, the mode is much broader, peaking at 1–2 μm.
- iron, for which both sites show a bimodal distribution. The most obvious difference is the coarse mode, which centres on 5 μm at PT and 2 μm at EROS, and parallels the behaviour of manganese. The mode at 2 μm seems likely due to brake dust, as that for Cu and Ba at EROS are at a similar size, close to that reported by Gietl et al. (2010) from a site in central London. The large peak at *ca* 5 μm for both Fe and Mn is most probably associated with emissions from the steelworks, based upon the much elevated concentrations observed at the PT site (see Fig. 3).

Components showing similar size modes, but different relative abundances were:

- particle mass, for which the fine mode was very similar at both sites, but the coarse mode was much more prominent at PT due largely to increased marine aerosol (Cl^-, Na^+, Mg^{2+}) and metallic elements, most notably Fe and Mn.
- coarse Cl^- and Na^+ from marine aerosol reflecting the proximity of the PT site to the sea.
- SO_4^{2-} and NH_4^+ which showed a greater abundance at the EROS site and are primarily associated with regional transport of secondary ammonium sulphate.
- NO_3^- is markedly coarser than ammonium at both sites, and a little finer than Cl^- and Na^+, consistent with an association with aged marine aerosol (Ottley and Harrison, 1992). Concentrations are higher at EROS, probably reflecting the east to west gradient in secondary nitrate and sulphate observed across the UK (AQEG, 2012), although the relatively short duration of sampling is insufficient to establish this beyond doubt.

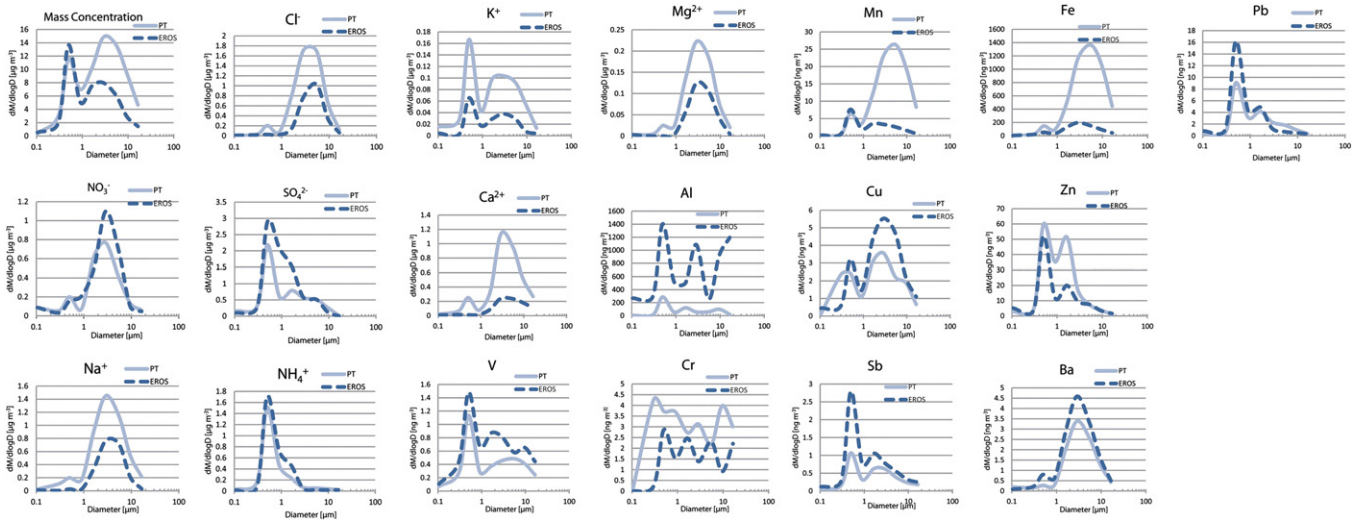

Fig. 3. Average MOUDI size distributions at the EROS and PT sites.

- K^+, which shows similar modes, but significantly higher concentrations at PT. Woodsmoke is usually the main source of fine K, while the coarse K may in part reflect marine aerosol, with also a likely contribution from steelworks emissions.
- coarse Ca^{2+} is also highly elevated at PT, probably reflecting emissions from steelworks processes and stockpiles.
- Al and V show elevated relative concentrations at EROS, probably reflective of soil/road dust as a source of Al (although the fine mode is hard to explain) and fuel oil combustion for V.
- Mn and Fe both show a much enhanced coarse mode at similar sizes at PT, consistent with a common steelworks source.
- Cu, Sb and Ba are all elements associated with brake wear emissions (Gietl et al., 2010). All appear to show a brake dust component at both sites —the mode at 3 μm is a characteristic (Gietl et al., 2010). In all cases, the data from EROS show higher concentrations. Published studies have reported Cu/Sb values of 4.6 and 5.3 for brake wear emissions (Sternbeck et al., 2002; Hjortenkrans et al., 2007). Studies on major roads have measured higher Cu/Sb values of 8.7–12 for fine and 10.5–13 for coarse particles (Song and Gao, 2011); and 9.1 (Gietl et al., 2010). In this study, these ratios were calculated to be 2.3, 7.2 and 3.7 (fine, coarse and PM_{10}) at EROS and 4.3, 5.4 and 4.9, respectively at PT. In the coarse mode the Cu/Sb ratio obtained at EROS was closer to Song and Gao (2011) and Gietl et al. (2010) consistent with a traffic influence. Cu, Sb, Pb and Zn all show a marked peak at 0.4–0.5 μm, probably associated with a higher temperature source, in the case of Cu, Sb and Pb most prominent at EROS.
- Zn shows modes at 0.4 μm and 2 μm which are more abundant at PT, especially the coarser mode. This is an element which as previously been associated with steelworks emissions (Dall'Osto et al., 2008).

Comparing the results of this study with the past work on MOUDI size distributions at PT reported by Dall'Osto et al. (2008), similarities were observed only for Fe, Pb and Zn, peaking at similar diameter. But unlike that study where Zn showed two peaks in the accumulation mode, only one peak was observed. Most of the elements reported in this study were not measured by Dall'Osto et al. (2008) besides a dissimilar modal peak measured for Cl^-. As for the EROS site, MOUDI size distributions for ionic and trace metal species have not previously been published. However, the work in the urban background (Regents College) in London by Gietl et al. (2010) could be expected to provide data comparable with EROS. Elements reported by Gietl et al. (2010) were Ba, Cu, Fe and Sb which are notable traffic markers. Except for Cu which exhibited two modal peaks, the EROS data were very similar to London for the other metals.

Braga et al. (2005) working in south Brazil found high enrichment factor values for Zn, Mn, Fe and Cr; and attributed the origin to steelworks. Pandolfi et al. (2011) have applied Positive Matrix Factorization (PMF) to source apportionment of particle samples from Gibraltar (Iberian Peninsula) and adopted Zn, Mn, Fe, and Cr as markers for the metallurgical industry. Mn, Fe and Zn emissions in Raahe (Finland) have been attributed to steel smelting by Oravisjarvi et al. (2003). Elevated coarse mode Ca at PT could have been emitted from steel production activities (Oravisjarvi et al., 2003). Ca can also emanate from construction processes especially in the coarse PM mode (Machemer, 2004; Ahn and Lee, 2006). The influence of soil dust and construction on the Ca emission has been assessed by Wang et al. (2005) using the Ca/Al ratio. A low value is indicative of soil dust while higher values indicate construction activities. The average Ca/Al ratios of 0.2 ± 0.3 and 8.1 ± 6.8 were obtained across MOUDI data (PM_{10}) at EROS and PT respectively. In the fine mode the values were 0.1 ± 0.1 (EROS) and 3.8 ± 3.3 (PT); while in the coarse mode the ratios were 0.4 ± 0.1 (EROS) and 13.5 ± 7.2 (PT). The far higher ratios of Ca/Al at PT are most likely attributable to an emission from the steelworks (see previous section), as the only major local construction activity related to earthworks associated with road building, particularly the Port Talbot Peripheral Distribution Road, which would be expected to cause an elevation in both elements.

Calculation of chloride depletion adopting the formula given by Zhao and Gao (2008) as % Cl = (1.81 × [Na] − [Cl]) / (1.81 × [Na]) × 100 for PM at EROS and PT gave 60 and 70% respectively. This Cl depletion value obtained at the PT site was similar to the study of Zhao and Gao (2008) who reported a Cl depletion value of 65% at a coastal site in the eastern US. Reaction of sea salt with atmospheric strong acids (HNO_3 and H_2SO_4) is the likely cause. The ratios again show a strong excess of coarse mode Ca at the PT site.

SO_4^{2+} and NH_4^+ appearing in the fine mode at 0.5–0.6 μm suggest formation of $(NH_4)_2SO_4$ or NH_4HSO_4 in the droplet mode. The droplet phase reaction involving oxidation of SO_2 to sulphate is very important in the atmosphere (Khoder, 2002). The modal peaks of 0.5 μm and a small mode between 1 and 2 μm observed for SO_4^{2-} at PT coinciding with those of Zn and Pb suggested internal mixing between SO_4^{2-} and Pb, and Zn. Formation of $PbSO_4$ and $ZnSO_4$ from the reactions involving Pb, Zn and SO_4 at the two modal sizes might have evolved from separate emission sources, which might be linked to the steelworks units or other anthropogenic activities. Previous studies at the steelworks have identified Pb and Zn as major emissions from the sinter and basic oxygen steel making sectors (Oravisjarvi et al., 2003; Dall'Osto et al., 2008).

At the PT site, Dall'Osto et al. (2008) found two peaks of Pb occurring at fine modes of 0.4–0.5 μm and 1–2 μm, which are similar to the modal peaks of Pb obtained in this study. Also, Dall'Osto et al. (2008) reported Zn to have a lone peak occurring at 1–2 μm relating to that obtained in this present study. However, another larger mode was found for Zn at 0.5 μm in this study. A small peak of SO_4^{2-} concentration in the coarse mode at 5.0 μm is suggestive of a reaction with mineral dust forming $CaSO_4$. The coarse mode Ca extended between 3 and 6 μm indicating internal mixing with coarse SO_4^{2-}. This may be an emission from the sinter process. Dall'Osto et al. (2008) reported different coarse modes for Fe dependent on the emission source. Such behaviour is also reflected in the size distributions for Fe seen in Fig. S4.

3.3. Data from specific sampling periods

3.3.1. Influence of wind conditions upon size distributions

Wind roses for the respective periods appear in Fig. S5.

3.3.1.1. Port Talbot. The periods showing the greatest mass concentrations in the coarse fraction (Fig. S3) are April 23–26, May 8–11 and May 5–8. All of these show a significant component to the wind rose in the southerly to westerly sector consistent with atmospheric transport from the steelworks. These periods also correspond to a major elevation in the concentrations of iron and manganese (Fig. S4). The period April 23–26 was also associated with high concentrations of zinc, barium, coarse vanadium, coarse calcium and coarse potassium, all of which have potential sources within the steelworks. The periods with the highest concentrations of coarse sodium and chloride was April 20–23 consistent with strong winds in the westerly sector transporting marine aerosol. The periods with the greatest association with the easterly wind sector were April 26–29, April 29–May 2 and May 2–5. The latter period was associated with high concentrations of nitrate, sulphate and ammonium, the secondary constituents whose concentrations are typically elevated in easterly air masses in the UK. Also elevated in this sample were concentrations of calcium and chloride with a mode at around 3 μm consistent with that of nitrate. This would appear to be due to transport of crustal calcareous material from the land masses to the east of Port Talbot which had collected nitrate and chloride from the vapour phase during their transport. Concentrations of iron and manganese were very low in these easterly samples.

Coarse particle modes for barium, antimony and copper, all constituents associated with automotive brake wear were notably elevated in the sample of April 17–20 consistent with a major automotive

contribution on winds from the north-west. This sample was also elevated in fine potassium suggesting a possible wood burning source also within this sector.

3.3.1.2. EROS site. The largest mass concentration in both the coarse and fine fractions was in the March 30–April 2nd sample which had the largest easterly wind component and intermediate wind speeds. The major ionic components exhibited their highest concentrations in this sample with ammonium and sulphate dominating the sub-micrometre fraction and chloride, nitrate and sodium, the coarse particle fraction. Concentrations of potassium, magnesium and calcium were also elevated in the coarse fraction in this sample. However, concentrations of the trace element constituents were in most cases relatively low in the sample of March 30–April 2 which is perhaps surprising given that the sample appears to contain a substantial continental component. The sample collected on April 5–8 stands out as having the highest concentrations of vanadium, manganese, copper, antimony and lead in the fine mode and of iron, manganese, barium and zinc in the coarse mode. The wind directions associated with the sample were predominantly in the sector from north-west to north-east corresponding to the Birmingham city centre and these constituents appear to be associated largely with non-tailpipe emissions from road traffic. The sample collected on April 8–11 associated with a predominant westerly wind component showed the lowest concentrations of nitrate, sulphate, ammonium, potassium and calcium suggesting relatively clean marine air on this westerly sector, although concentrations of the marine indicator elements chloride and sodium were not particularly elevated. An interesting feature of the EROS dataset is that the ranking of concentrations between the samples for fine fraction potassium was the same as that for sulphate. Since the latter is well known as a pollutant subject to regional transport, this suggests that fine potassium, whose main source is believed to be woodsmoke (Harrison et al., 2012b), is also subject to long-range transport in a broadly similar manner. Other constituents which showed identical or similar rankings of concentration to one another (but not to sulphate and potassium) were vanadium, manganese, iron, antimony, barium and lead suggesting a common source for most elements, most probably in non-tailpipe emissions from road traffic.

3.4. Coarse particle increment at Port Talbot

The measured data are insufficient to conduct a mass closure on the aerosol composition, but it is nonetheless instructive to examine the differences in coarse particle mass and composition between PT and EROS (see Table S1). The difference in coarse particle ($PM_{2.5-10}$) mass between the sites is 6.1 μg m^{-3}. Marine aerosol (taken as Na^+, Cl^- and Mg^{2+}) accounts for just 1.0 μg m^{-3} of this. Elements thought to be associated with steelworks (Fe and Ca^{2+}) together amount to 1.6 μg m^{-3}, which may approximately double to 3.2 μg m^{-3} when associated elements are added (e.g. Fe_2O_3 and $CaCO_3$). This suggests that under the conditions sampled, steelworks-related emissions account for at least half of the elevation in $PM_{2.5-10}$. The mass unaccounted for of *ca* 2 μg m^{-3} may be attributable to carbonaceous emissions, for example from the coke ovens, but data were not collected allowing this to be tested.

3.5. Analysis of particle size spectra collected with the Grimm optical spectrometer

The Grimm instrument has a response time of seconds, and in order to obtain statistically significant counts, the data were averaged over hourly periods and were then plotted as polar plots as a function of wind direction and wind speed. The data are collected in 14 separate size bins and polar plots for each size bin appear in Fig. S6 in the Supplementary information. Fig. 4 shows the polar plots for four of the size classes which give a good representation of the overall behaviour observed.

In the case of $PM_{0.4-0.5}$ (see Fig. 4) the highest concentrations are associated with all wind sectors and very low wind speeds (the red area in the centre of the plot). This is indicative of a local ground-level source with maximum concentrations under low wind speed conditions. This we attribute to local road traffic. This behaviour is also seen for $PM_{0.3-0.4}$ and to a lesser extent for the $PM_{0.5-0.65}$ plot. For sizes between

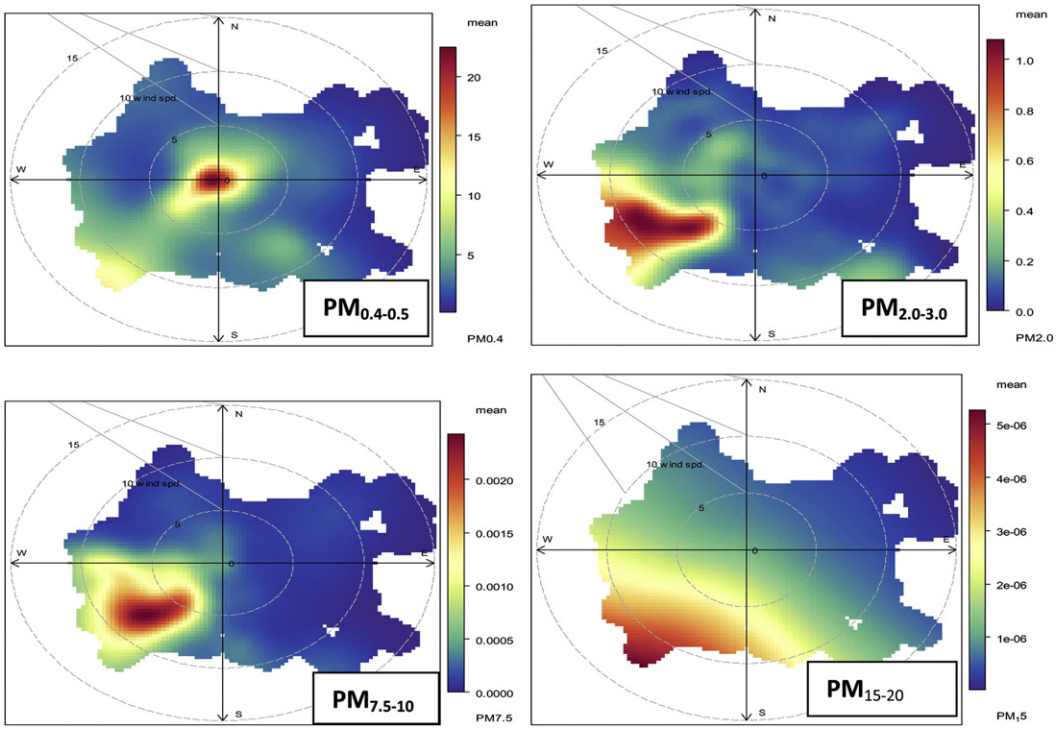

Fig. 4. Polar plots of particle number count in selected size bins as a function of wind direction and speed.

$PM_{0.5–0.65}$ and $PM_{5.0–7.5}$, the behaviour is very similar for each size fraction and is exemplified by the plot for $PM_{2.0–3.0}$ in Fig. 4. This indicates a source area on a sector between 200° and 250° and intermediate wind speeds of 5–10 m s^{-1}, extending to the highest observed wind speeds of >10 m s^{-1} for particle sizes of $PM_{2.0–3.0}$ and below to $PM_{0.5–0.65}$. The association with the highest wind speeds becomes much less strong and the plot for $PM_{7.5–10}$ (Fig. 4) shows a strong association with the intermediate wind speeds. The directional association of this peak clearly links it with sources within the steelworks and the association with intermediate wind speeds strongly suggests an elevated source. A ground-level emission source would most likely give peak concentrations at lower wind speeds (as for road traffic) and a resuspension source would be associated primarily with the highest wind speeds. Consequently, the data for particle sizes between the $PM_{0.5–0.65}$ and $PM_{2.0–3.0}$ plots appear to be a combination of both the elevated source and the ground-level resuspension source while the plots from $PM_{3.0–4.0}$ to $PM_{10–15}$ are indicative of an influence predominantly from the elevated sources.

The plot for $PM_{7.5–10}$ gives a very clear indication of a predominant emission at intermediate wind speeds on the south-westerly sector (i.e. centred on 225°) which is the direction associated with the sinter plant and blast furnace within the steelworks. For the highest particle

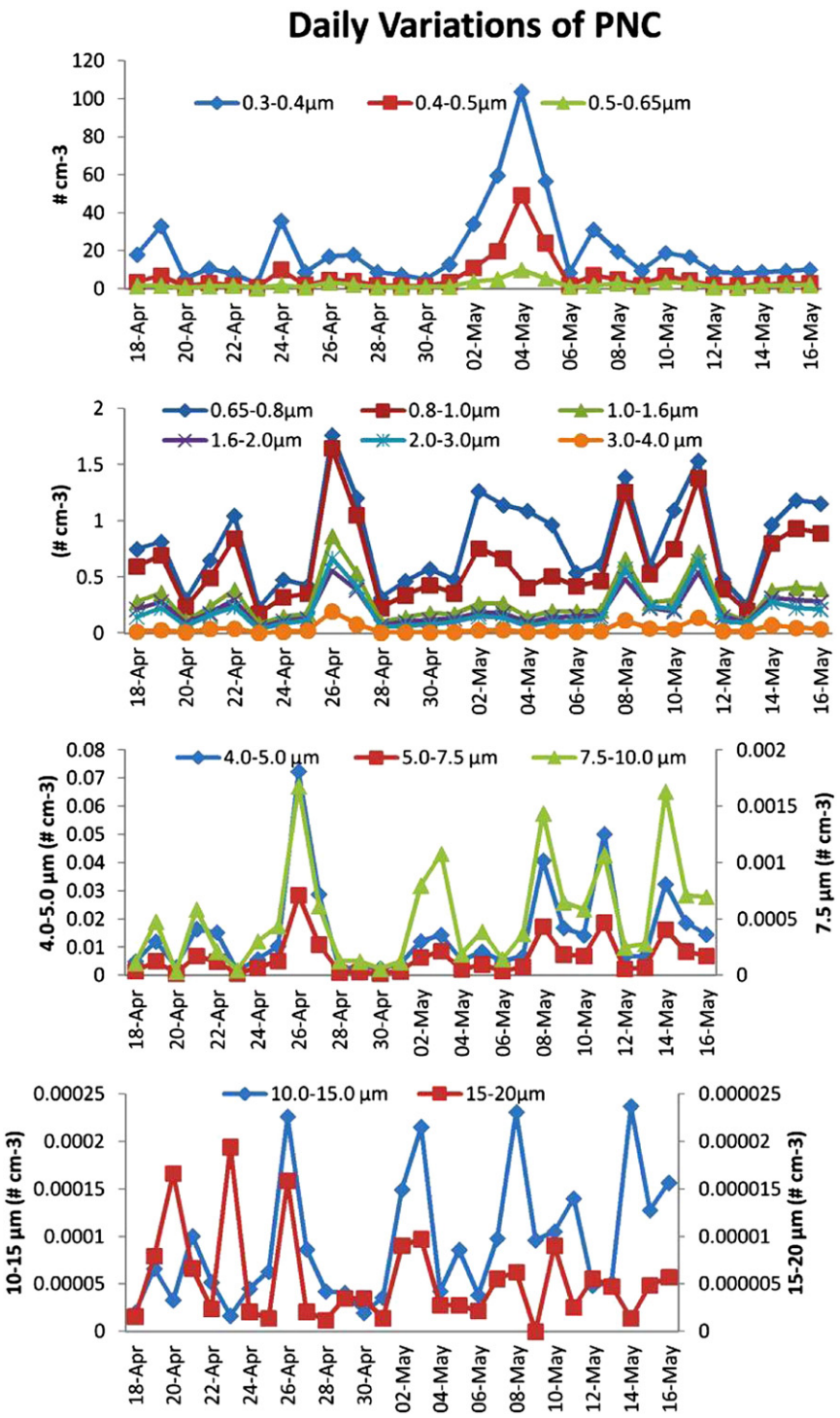

Fig. 5. Diurnal variations of PM size ranges as PNC (particle number concentration).

size bin (PM_{15-20}) the polar plot (Fig. 4) has changed to one focussed heavily on the strongest wind speeds and also covering a wider range of wind sectors strongly suggestive of a marine source (O'Dowd and de Leeuw, 2007), possibly supplemented by resuspension from within the steelworks as indicated by the highest concentrations on the south-westerly sector.

It would be useful to look for associations between the modes in the MOUDI size distributions and the peaks in the polar plots for different particle sizes. This is, however, made difficult by the lack of a clear relationship between optical diameters measured by the Grimm spectrometer and aerodynamic diameters measured by the MOUDI. The elements showing far the greatest elevation at PT over EROS are Fe and Mn (Fig. 3) with a mode at around 5 μm, extending from *ca* 2 to 10 μm aerodynamic diameter. This appears to be associated with the major peak in the polar plots at around 225° appearing for particles in size ranges from 0.3–3.0 μm to 10–15 μm (Fig. S7). The two datasets therefore appear broadly consistent.

The daily variations of particle number concentrations (PNC) are shown in Fig. 5. Notable episodes were observed for all the particle size bins on April 26, May 3–4, 8 and 11. These peaks correspond to episodes of PM_{10} pollution observed by the Partisol and FDMS instruments. On April 26 and May 11, both measuring instruments recorded PM_{10} mass concentrations greater than the European Union 24-hr limit of 50 μg m^{-3} while on May 8, the values of PM_{10} mass were greater than 40 μg m^{-3}. Particles between 0.3 and 0.5 μm revealed elevated concentrations on May 4 in which a sharp decline was observed for other particle bins except $PM_{0.5-0.65}$. For particles in size bins from 0.65 to 7.5 μm, similar emission patterns were observed with highest peak shown on April 26. Significant peaks were also shown on May 2–3, 8, 11 and 15. To some extent, levels of agreement were seen in the daily emission trends of particles with diameters 10–15 μm and 0.65–7.5 μm while particles between 15 and 20 μm revealed different emission patterns. As discussed earlier, $PM_{0.3-0.5}$ is dominated by vehicular emissions; $PM_{0.8}$ to PM_{10} were more influenced by the steelworks while PM_{15-20} is strongly affected by marine particles.

It is instructive to examine the sources of PNC in response to meteorology on the days of episodes shown as April 26, May 4, 8 and 11 (Fig. S6). On April 26, between 12 pm and 2 am, the prevailing wind was between 200° and *ca* 300° where the ironmaking section of the steelworks was located. At the windspeed of 8 m s^{-1}, it appeared that PNC of all the particle size bins are favoured by the elevated windspeed due to effective transport from the point source (the steelworks) to receptor site. As the windspeed increases to about 10 m s^{-1}, there was a drastic reduction in particle number concentrations due to a dilution effect (Charron and Harrison, 2005). There was an increase in concentration of $PM_{0.3-0.4}$ when the windspeed reduced at around 6 am. Over this period, the prevailing wind direction has shifted to the south-easterly where the M4 road linking South Wales to London was located. Elevated particle concentrations of size bins 0.3 to 0.5 μm at 6 am may therefore be linked to traffic emission favoured by low windspeed and/or low dispersion.

On May 4, the major particle increment was in the smaller size bins and probably due to an elevation in secondary particle concentrations. Elevated particle numbers were favoured at a moderate windspeed 4–5 m s^{-1}. When the windspeed began to increase, PNC also reduced with a change of wind direction. The situation on May 8 and 11 looks similar to that of April 26, with the elevated values of PNC (sizes > 0.65 μm) from the steelworks under a moderate windspeed. However, with a change of wind direction and speed; particles <0.65 μm increased between 6 and 10 am probably due to traffic emissions.

4. Conclusions

This study has revealed distribution patterns of size-segregated particles at a typical urban background (EROS) and an industrial setting (Port Talbot). Individual sample and average MOUDI data presented were diverse and varied between the two sites. EROS was dominated by fine particles while PT showed an elevated coarse particle concentration reflected in a higher ratio of $PM_{2.5}/PM_{10}$ obtained at EROS. The influence of secondary aerosol was more evident at the urban background than the industrial site. Port Talbot showed elevated concentrations of marine (Na^+, Mg^{2+} and Cl^-) and steelworks emissions (Fe, Mn and Ca). Higher concentrations of trace metals such as V, Al and Pb were observed at EROS. Strong similarities in mass size distributions were observed between Mn and Fe at PT (this was not so at EROS) suggesting a common emission source from the steel industry. Trace metals associated with brake wear (Cu, Sb, Ba) were clearly observed at both sites.

The analysis of size distributions from individual 72-hour sampling intervals confirmed the inferences derived from the average data, but allowed some appreciation of the episodicity of contributions both from the steelworks and secondary particles. Both showed the expected associations with, in the former case local winds from the direction of the steelworks, and easterly sector winds associated with regional transport in the latter. Although containing no chemical information, the polar plots of particle number size spectra revealed much source-related information. Local emissions, probably from road traffic dominated the smaller size bins (0.3–0.5 μm), while steelworks emissions dominated the range 0.5–15 μm, and for particles >15 μm marine aerosol appeared dominant. Although there appeared to be contributions from more than a single source within the steelworks, the wind direction-dependence suggested the sinter plant and/or blast furnaces as the major contributor.

Conflict of interest

The authors have no actual or potential conflict of interest including any financial, personal or other relationships with other people or organizations within three years of beginning the submitted work that could inappropriately influence, or be perceived to influence, their work.

Acknowledgements

We are grateful for support from the the National Centre for Atmospheric Science (NCAS) which is funded by the UK Natural Environment Research Council and for support to Adewale Taiwo from the Tertiary Education Trust Fund (TETFund), Federal University of Agriculture, Abeokuta, Nigeria. Furthermore, we would like to formally thank Neath-Port Talbot Council, the Environment Agency Wales, Mid and West Wales Fire and Rescue Service, Dwr Cymru and Dyffryn School, Port Talbot for hosting our measurements.

Appendix A. Supplementary data

Supplementary data to this article can be found online at http://dx.doi.org/10.1016/j.scitotenv.2013.12.076.

References

Ahn YC, Lee JK. Physical, chemical, and electrical analysis of aerosol particles generated from industrial plants. Aerosol Sci 2006;37:187–202.
Allen AG, Nemitz E, Shi JP, Harrison RM, Greenwood JC. Size distributions of trace metals in atmospheric aerosols in the United Kingdom. Atmos Environ 2001;35:4581–91.
AQEG, Air Quality Expert Group. Understanding PM_{10} in Port Talbot. Northern Ireland: Advise note prepared for Department of Environment, Food and Rural Affairs: Scottish, Welsh Assembly Government, and Department of the Environment; 2011 [uk-air.defra.gov.uk/…/110322_AQEG_Port_Talbot_Advice_Note.pd. Accessed on 04/01/13].
AQEG. Fine particulate matter ($PM_{2.5}$) in the United Kingdom. London: Air Quality Expert Group, Department for Environment, Food and Rural Affairs; 2012.
Braga CF, Teixeira EC, Meira L, Wiegand F, Yoneama ML, Dias JF. Elemental composition of PM10 and PM2.5 in urban environment in South Brazil. Atmos Environ 2005;39:1801–15.
Cabada JC, Rees S, Takahama S, Khlystov A, Pandis SN, Davidson CI, et al. Mass size distributions and size resolved chemical composition offline particulate matter at the Pittsburgh supersite. Atmos Environ 2004;38:3127–41.

Chang L-P, Tsai J-H, Chang K-L, Lin JJ. Water-soluble inorganic ions in airborne particulates from the nano to coarse mode: a case study of aerosol episodes in southern region of Taiwan. Environ Geochem Health 2008;30:291–303.
Charron A, Harrison RM. Fine ($PM_{2.5}$) and coarse ($PM_{2.5-10}$) particulate matter on a heavily trafficked London highway: sources and processes. Environ Sci Technol 2005;39:7768–76.
Dall'Osto M, Booth MJ, Smith W, Fisher R, Harrison RM. Study of the size distributions and the chemical characterization of airborne particles in the vicinity of a large integrated steelworks. Aerosol Sci Technol 2008;42:981–91.
Figueroa DA, Rodrıguez-Sierra CJ, Jimenez-Velez BD. Concentrations of Ni and V, other heavy metals, arsenic, elemental and organic carbon in atmospheric fine particles (PM2.5) from Puerto Rico. Toxicol Ind Health 2006;22:87–99.
Gietl JK, Lawrence R, Thorpe AJ, Harrison RM. Identification of brake wear particles and derivation of a quantitative tracer for brake dust at a major road. Atmos Environ 2010;44:141–6.
Harrison RM, Tilling R, Callen Romero MS, Harrad S, Jarvis K. A study of trace metals and polycyclic aromatic hydrocarbons in the roadside environment. Atmos Environ 2003a;37:2391–402.
Harrison RM, Jones AM, Lawrence RG. A pragmatic mass closure model for airborne particulate matter at urban background and roadside sites. Atmos Environ 2003b;37:4927–33.
Harrison RM, Jones A, Gietl J, Yin J, Green D. Estimation of the contribution of brake dust, tire wear and resuspension to nonexhaust traffic particles derived from atmospheric measurements. Environ Sci Technol 2012a;46:6523–9.
Harrison RM, Beddows DCS, Hu L, Yin J. Comparison of methods for evaluation of wood smoke and estimation of UK ambient concentrations. Atmos Chem Phys 2012b;12:8271–83.
Hjortenkrans DST, Bergback BG, Haggerud AV. Metal emissions from brake linings and tires: case studies of Stockholm, Sweden 1995/1998 and 2005. Environ Sci Technol 2007;41:5224–30.
Jones AM, Harrison RM, Baker J. The wind speed dependence of the concentrations of airborne particulate matter and NO_x. Atmos Environ 2010;44:1682–90.
Khoder MI. Atmospheric conversion of sulphur dioxide to particulate sulphate and nitrogen dioxide to particulate nitrate and gaseous nitric acid in an urban area. Chemosphere 2002;49:675–84.
Kleeman MJ, Schauer JJ, Cass GR. Size and composition distribution of fine particulate matter emitted from motor vehicles. Environ Sci Technol 2000;34:1132–42.
Liu S, Hua M, Slaninaa S, Heb L-Y, Niub Y-W, Bruegemann E, et al. Size distribution and source analysis of ionic compositions of aerosols in polluted periods at Xinken in Pearl River Delta (PRD) of China. Atmos Environ 2008;42:6284–95.
Machemer SD. Characterization of airborne and bulk particulate from iron and steel manufacturing facilities. Environ Sci Technol 2004;38:381–9.
Moreno T, Jones TP, Richards RJ. Characterisation of aerosol particulate matter from urban and industrial environments: examples from Cardiff and Port Talbot, South Wales, UK. Sci Total Environ 2004;334–335:337–46.
Ny MT, Lee BK. Size distribution of airborne particulate matter and associated metallic elements in an urban area of an industrial city in Korea. Aerosol Air Qual Res 2011;11:643–53.
O'Dowd CD, de Leeuw G. Marine aerosol production: a review of the current knowledge. Phil Trans R Soc 2007;365:1753–74.
Oravisjarvi K, Timonen KL, Wiikinkoski T, Ruuskanen AR, Heinanen K, Ruuskanen J. Source contributions to PM2.5 particles in the urban air of a town situated close to a steel works. Atmos Environ 2003;37:1013–22.
Ottley CJ, Harrison RM. The spatial distribution and particle size of some inorganic nitrogen, sulphur and chlorine species over the North Sea. Atmos Environ 1992;26A:1689–99.
Pandolfi M, Gonzalez-Castanedo Y, Alastuey A, de la Rosa J, Mantilla E, Sanchez de la Campa A, Querol X, Pey J, Amato F, Moreno T. Source apportionment of PM10 and PM2.5 at multiple sites in the strait of Gibraltar by PMF: impact of shipping emissions. Environ Sci Pollut Res 2011;18:260–9.
Samara C, Kouimtzis Th, Tsitouridou R, Kanias G, Simeonov V. Chemical mass balance source apportionment of PM10 in an industrialized urban area of Northern Greece. Atmos Environ 2003;37:41–54.
Song F, Gao Y. Size distributions of trace elements associated with ambient particular matter in the affinity of a major highway in the New Jersey–New York metropolitan area. Atmos Environ 2011;45:6714–23.
Sternbeck J, Sjodin A, Andreasson K. Metal emissions from road traffic and the influence of resuspension —results from two tunnel studies. Atmos Environ 2002;36:4735–44.
Wang Y, Zhuang G, Tang A, Yuan H, Sun Y, Chen S, et al. The ion chemistry and the source of PM2.5 aerosol in Beijing. Atmos Environ 2005;39:3771–84.
Wood Protection Association. Use of CC-treated timber. A Wood Protection Association Guidance note. www.ttf.co.uk/Document/Default.aspx?DocumentUid, 2010. [A063 Accessed 29/12/12].
Xia L, Gao Y. Chemical composition and size distributions of coastal aerosols observed on the US East Coast. Mar Chem 2010;119:77–90.
Yin J. Harrison, RM. Pragmatic mass closure study for $PM_{1.0}$, $PM_{2.5}$ and PM_{10} at roadside, urban background and rural sites. Atmos Environ 2008;42:980–8.
Yin J, Harrison RM, Chen Q, Rutter A, Schauer JJ. Source apportionment of fine particles at urban background and rural sites in the UK atmosphere. Atmos Environ 2010;44:841–51.
Zanobetti A, Franklin M, Koutrakis P, Schwartz J. Fine particulate air pollution and its components in association with cause-specific emergency admissions. Environ Health 2009;8:58. http://dx.doi.org/10.1186/1476-069X-8-58.
Zhao Y, Gao Y. Acidic species and chloride depletion in coarse aerosol particles in the US east coast. Sci Total Environ 2008;407:541–7.